



## Wear of potential tool materials for aluminium alloys friction stir welding at weld temperatures

Mart Kolnes<sup>\*</sup>, Jakob Kübarsepp, Fjodor Sergejev, and Märt Kolnes

Department of Mechanical and Industrial Engineering, Tallinn University of Technology, Ehitajate tee 5, 19086 Tallinn, Estonia

Received 31 January 2019, accepted 20 March 2019, available online 24 April 2019

© 2019 Authors. This is an Open Access article distributed under the terms and conditions of the Creative Commons Attribution-NonCommercial 4.0 International License (<http://creativecommons.org/licenses/by-nc/4.0/>).

**Abstract.** Friction stir welding is a solid-state joining process that uses a non-consumable tool to join materials by mixing them mechanically in the weld area instead of melting them. The high-quality friction stir welding (FSW) process temperatures are in the range of 400–500 °C. Adhesive wear is suggested to be the main wear mechanism for the FSW tool. Adhesive wear testing should be performed at the weld temperature or close to the welding process temperatures for better simulation of real-life FSW tool wearing conditions. Adhesive wear tests of three FSW tool materials, WC–Co and TiC based with NiMo and FeCr binders at temperatures of 70 °C (low) and 400 °C (high) were performed by turning aluminium alloy AW6082-T6. The higher temperature in the cutting zone was achieved by increasing the cutting speed. To measure the temperature at the interface of the cutting tool and the workpiece, a novel method based on the thermoelectric effect was used. The wear was determined as the change of the geometry of the cutting edges of the tool. Microscopic investigations were performed by using scanning electron microscopy. The distribution of chemical elements and the chemical composition of the tool cutting edge were analysed by energy dispersive X-ray spectroscopy. The TiC-based cermets (TiC–NiMo and TiC–FeCr) demonstrated superiority over WC–Co cemented carbide at both low (70 °C) and high (400 °C) temperatures. The highest wear performance at the low temperature was shown by the Fe-alloy bonded composite TiC–FeCr while at the high temperature the Ni-alloy bonded cermet TiC–NiMo had the highest wear performance.

**Key words:** friction stir welding, cermet, cemented carbide, adhesive wear, weld temperature.

### 1. INTRODUCTION

Friction stir welding (FSW) is a thermomechanical deformation joining process that uses a specially designed tool to join materials without melting them [1,2]. The FSW tool serves three primary functions: heating of the workpiece, movement and mixing of the material to produce the joint, and containment of the hot metal beneath the tool shoulder. Heating is produced within the workpiece both by friction between the rotating tool pin and the shoulder and by severe plastic deformation

of the workpiece [3]. Localized heating softens the material around the pin. As a result of the tool rotational action and the influence on the workpiece, if performed properly, a qualitative solid-state joint is produced. It is essential to ensure that the tool will not lose special features, such as the geometry of the pin, and/or texture features of the shoulder part of the tool and dimensional stability by the wear at weld temperature.

Excessive tool wear changes the tool shape (normally by removing tool features), thus changing the weld quality and increasing the probability of defects. In friction stirring, tool wear can occur due to adhesive, abrasive, or chemical wear (addressed subsequently as reactivity)

<sup>\*</sup> Corresponding author, [mart.kolnes@taltech.ee](mailto:mart.kolnes@taltech.ee)

mechanisms. The exact wear mechanism depends on the interaction between the workpiece and the tool material and the selected tool parameters [4].

The cemented carbides and cermets selected for our study as prospective FSW tool materials have relatively high abrasive wear resistance as compared to common tool materials [5,6]. For this reason, we concentrated on the adhesive wear of these materials. Previous adhesive wear studies at room temperature have shown that TiC-based cermets are of great potential in FSW applications [7]. For better simulation of real-life welding conditions, the adhesive wear was studied at temperatures close to the weld temperatures.

It is well known that temperature may influence the wear mechanism [8]. Generally, this is attributed to the decreased yield strength and increased ductility at elevated temperatures. Gåård et al. investigated the effect of frictional heating on the adhesive wear mechanism [9]. They claimed that adhesive wear is influenced by temperature, as increased temperature leads to shorter sliding distances until the onset of severe wear, distinguished as an increase of the coefficient of friction. They found that the transition to severe adhesive wear occurs at similar sliding distances for similar temperatures, although the normal loads and velocities are different. They assumed that the very high sensitivity of adhesive wear to temperature already at lower temperatures is unlikely to depend on the change in mechanical properties. Tang et al. found that the highest temperature in the welding seam is approximately 0.8 of the melting temperature of the welded material [10].

The FSW tool is commonly coated by a layer of weldable material, in particular an aluminium alloy. The problem here is that the generation of the tribological layer on the tool surface creates conditions for the diffusion of elements into the tool metal. A rationale behind the tool wear in the FSW of aluminium alloys could be strong adhesion of the aluminium alloy to a tool and the following diffusion of the tool material into aluminium due to high temperatures developed during welding [11]. The reaction-diffusion of iron into aluminium is a well-known phenomenon that has been observed in many cases [12]. Hirano et al. investigated the diffusion of iron, nickel, and cobalt in aluminium at a temperature range over 360 to 630 °C and measured

the temperature dependences of diffusivities of these materials in aluminium [13].

Currently, the most often used method to measure cutting temperature is the tool–workpiece thermocouple method, which uses Seebeck’s principle. Previous studies have proved that a metal subjected to a temperature differential undergoes a non-uniform distribution of free electrons, which subjects this metal to an electromotive force differential [14]. This method requires two different metals joined in one part. Along the paths of the thermocouple circuit, the electromotive force is given by the product of the difference between the Seebeck’s coefficients of thermocouple materials and the temperature gradient between the closed and open junctions of the thermocouple. With the tool–workpiece thermocouple method, the amount of electromotive force is an indication of the average temperature in the tool–workpiece interface. On certain occasions, the electromotive force does not correspond to the average cutting temperature of the interface; it only corresponds in the cases when the temperature is uniform, or if the thermoelectric obtained from the tool–workpiece combination varies linearly along with the cutting temperature. The tool–workpiece thermocouple method was recently used also for measuring the FSW process temperature [15].

This work focuses on the performance of carbide composites in wear conditions with the prevalence of adhesion at a low and near weld temperature during the FSW of an aluminium alloy.

## 2. EXPERIMENTAL DETAILS

Wear tests at different temperatures were performed on a universal lathe. The aluminium alloy AW6082-T6 (1.1% Si, 0.5% Mn, 0.8% Mg, rest Al) round bar of 200 mm diameter was machined at high speeds, up to 630 m/min. Three different cutting tool materials were used. The composition of carbide-based composites and their mechanical properties are presented in Table 1.

The carbide volume content was calculated taking into account the dissolution of Mo in TiC and the formation of secondary Cr-based carbides in cermets TiC–NiMo and TiC–FeCr, respectively. Microstructures of carbide composites are shown in Fig. 1. The TiC–FeCr

**Table 1.** Composition and mechanical properties of carbide composites

Designation	Initial composition, wt%		Carbide content, vol%	Hardness HV30	Fracture toughness, MPa·m <sup>1/2</sup>
	Carbide	Binder			
WC–Co	85 WC	Co(W) 15	76.4	1100 ± 20	17.8 ± 0.5
TiC–NiMo	75 TiC	Ni 16.7, Mo 8.3	89.9	1378 ± 25	11.4 ± 0.4
TiC–FeCr	70 TiC	Fe 25.8, Cr 5.1	84.0	1225 ± 6	10.2 ± 0.7

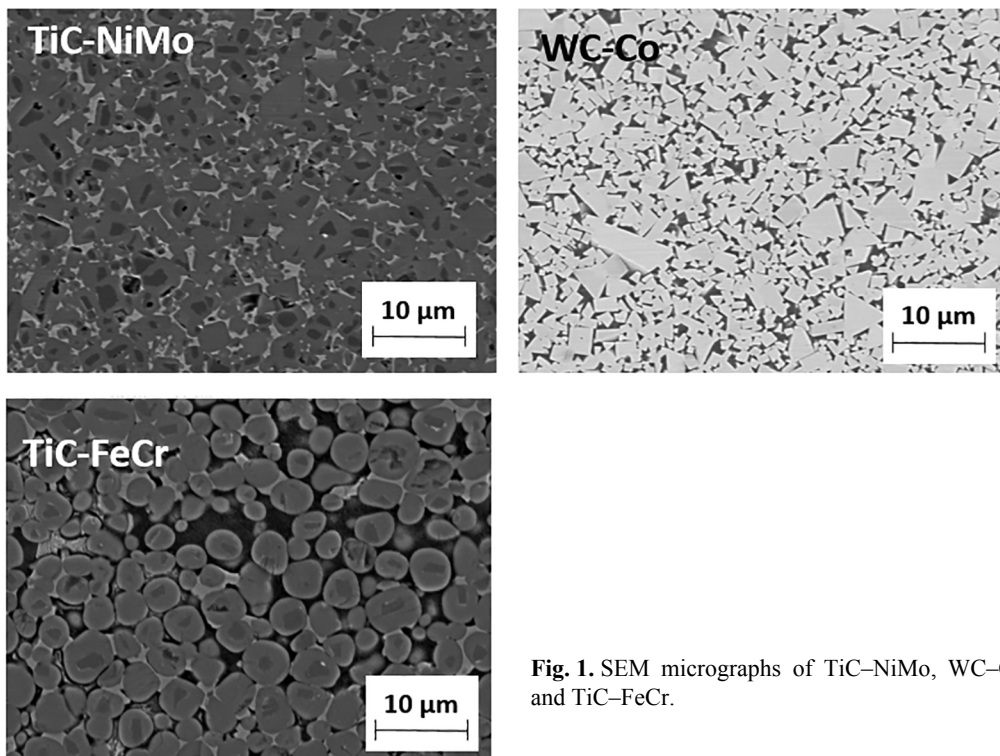


Fig. 1. SEM micrographs of TiC–NiMo, WC–Co, and TiC–FeCr.

cermet was etched in nitric acid 5% solution for 90 s to determine its carbide volume content, for which image analysis software OmniMet was used.

To measure the cutting temperature in the cutting point, a tool–workpiece thermocouple system was used

[16]. The scheme of this system is presented in Fig. 2. The workpiece and the turning tool were insulated from the lathe. The cold end of the tool and the three-bush device were connected to the voltmeter to measure the electromotive force.

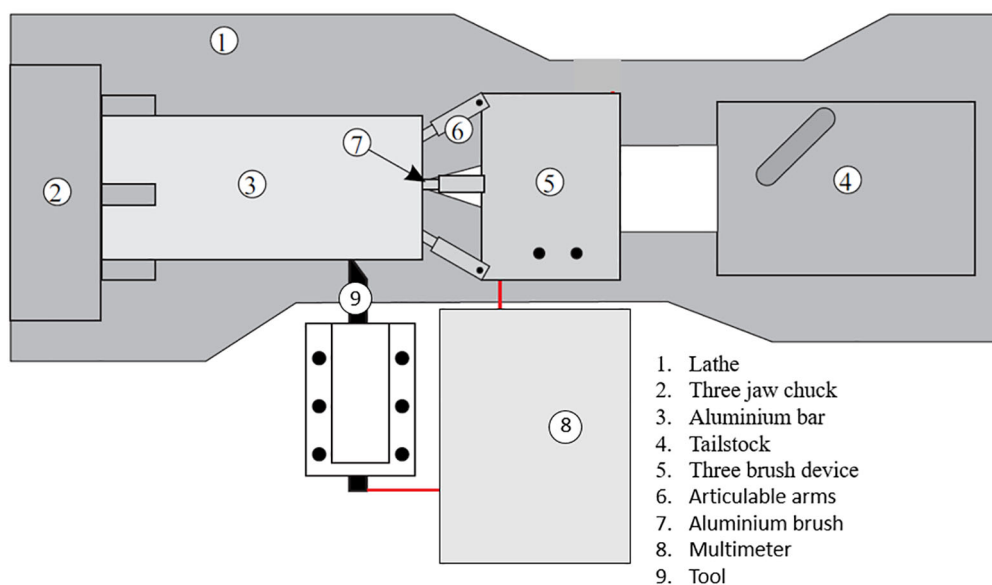


Fig. 2. Schematic of the tool–workpiece thermocouple system (top view) [16].

To ensure reliable temperature measurements, the tool–workpiece thermocouple must be the only high-temperature point in the system. All the other material connections have to be at room temperature. To maintain the electrical conductivity in the tool–workpiece thermocouple circuit during the turning of the aluminium alloy, a three-brush device was used. The main function of the three-brush device is to maintain the electrical continuity of the tool–workpiece thermocouple circuit with the workpiece in rotational movement. The device used is similar to that of Santos et al. [16].

In this work, calibrations of the tool–workpiece thermocouple were carried out with tool materials under research. Long bars of the tool materials were prepared with one end joined with an aluminium chip. The calibration thermocouples were introduced into an electrical furnace and heated up to 500 °C. The electromotive force was measured on the outside ends of the ceramic-based composite bar and the aluminium chip, which were at room temperature. Therefore, the electromotive force was dependent only on the temperature of the contact point between the composite and the aluminium chip. Figure 3 shows the calibration curves of the two tested thermocouple materials.

The electromotive force was 6.1 mV, 2.4 mV, and 1.9 mV for WC–Co, TiC–FeCr, and TiC–NiMo, respectively, at 440 °C, which is close to the maximum FSW temperature of aluminium alloy AW6082-T6. Three measurements were performed for each specimen, and the results of the temperature measured by the three-brush device are average values.

To investigate the dependence of cutting temperature on the cutting speed in the case of the cemented carbide, WC–Co tool turning tests were performed at cutting speeds up to 630 m/min. Raising the cutting speed over 500 m/min did not increase the temperature significantly (Fig. 4). The reason is that for our lathe test setup, the temperature of the cutting tool in contact stabilizes at around 410 °C. Although the approximate

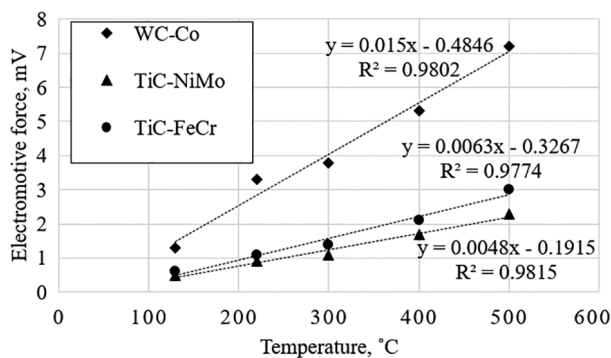


Fig. 3. Relationship between the temperature and the electromotive force for ceramic-based materials tested.

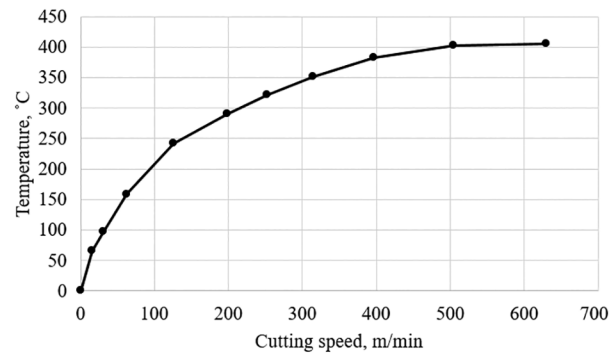


Fig. 4. Cutting speed vs cutting point temperature in the case of the WC–Co tool.

welding temperature of the aluminium alloy AW6082-T6 is about 440 °C, it was not reached during the turning tests. Therefore, 500 m/min was selected as the cutting speed for adhesive wear tests in the case of WC–Co cemented carbide. The same cutting speed to achieve the cutting temperature of approximately 400 °C was also used for the tools made from cermets. The cutting speed of 17 m/min was used in tests at low-temperature (approximately 70 °C) wear conditions.

The cemented carbide and cermets tools were ground in order to achieve a nose angle of 134°, side cutting-edge angle of 23°, and side relief angle of 8°. The total cutting distance for each specimen was 4400 m. The feed rate and the depth of cut were kept constant during testing at 0.39 mm/rev and 0.125 mm, respectively. Changes in the geometry of the specimens were measured using the images made from the top surface of the cutting tool by Hitachi TM 1000 Tabletop scanning electron microscope. The adhesion wear rate was determined as the shortening (in  $\mu\text{m}$ ) in the length of the cutting nose tip of the specimen. Measurements were performed at certain distances (1100, 2200, and 4400 m) and before each measurement, the specimen was cauterized (to make nose tip measurements) using a sodium hydroxide solution (NaOH 20 wt%). In order to understand the distribution of chemical elements in the microstructure in the tool–workpiece contact region, the energy-dispersive X-ray spectroscopy (EDS) system INCA was used.

### 3. RESULTS AND DISCUSSION

Previous research [17–19] has shown that at similar volume fraction of carbides TiC-based cermets independent of their binder composition and structure are at a disadvantage compared to WC-based cemented carbides in abrasive erosion and also in abrasive wear conditions. The performance of carbide composites in

abrasion conditions is controlled primarily by the stiffness of the composite, i.e. its resistance to elastic (evaluated by the modulus of elasticity) and plastic (evaluated by proof stress) strains, and depends chiefly on the properties of the carbide phase (WC vs TiC) [17,18]. At the same time, the adhesive wear performance of cermets may be comparable to that of WC-based composites, as it is controlled primarily by composite resistance to plastic strain featured by the proof stress that depends on properties of both the metallic and the ceramic phase [17,19].

In the present research TiC-based composites (cermets) demonstrated superiority over WC-based cemented carbides at both low (70 °C) and elevated (400 °C) temperatures (*see* Table 2 and Fig. 5). The high

wear performance of TiC-based cermets indicates that the prevailing mechanism in the wear testing conditions used in the present research was adhesion. At the low temperature, the highest wear performance was demonstrated by the TiC–FeCr cermet while at the high temperature the TiC–NiMo cermet outperformed both WC–Co and TiC–FeCr composites (Fig. 5, Table 2).

The wear performance of cermet, bonded with the Ni alloy (TiC–NiMo) as distinct from WC–Co and TiC–FeCr composites appeared to be similar at low (70 °C) and elevated (400 °C) temperatures. In other words, the wear temperature sensitivity of the Ni-alloy bonded cermet was markedly lower compared to the other carbide composites investigated.

Figure 5 demonstrates wear performance plotted against the cutting distance at two different temperatures of the WC–Co cemented carbide and TiC–FeCr and TiC–NiMo cermets. Increase in the temperature resulted in a marked growth of wear, i.e. shortening of the cutting nose tip (except the TiC–NiMo cermet). At the same time different composites demonstrated no marked differences in the wear gain rate during the increase of the cutting distance: the wear rate increase angles ( $\alpha$ ,  $\beta$ , and  $\gamma$ ) were almost similar at different temperatures (*see* Fig. 5).

**Table 2.** Cutting tool nose tip shortening for tested materials at the final cutting distance of 4400 m

Material	Shortening of the cutting nose tip, $\mu\text{m}$	
	at 70 °C	at 400 °C
WC–Co	3.9	5.5
TiC–NiMo	3.6	3.3
TiC–FeCr	2.4	4.5

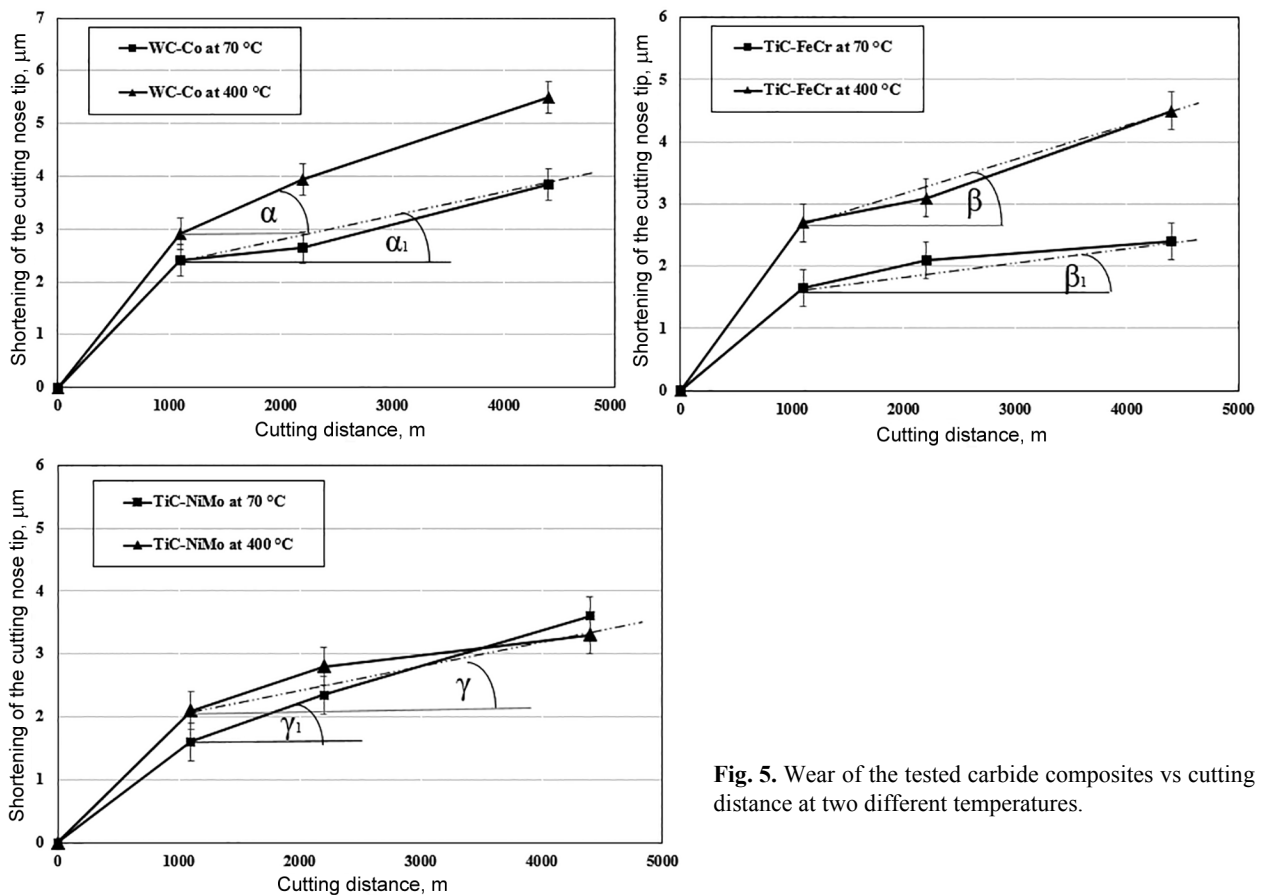


**Fig. 5.** Wear of the tested carbide composites vs cutting distance at two different temperatures.

The SEM studies (Fig. 6) demonstrated failure (material removal) of the cutting tool tip after the wear tests of carbide composites. Micrographs confirm our previous research results of adhesive wear performance of cemented carbides and cermets [19]. The structure of the worn cutting nose tip is distinctive, proving that adhesive failure starts preferably in the binder continuing by the extraction of carbides.

Figure 7a shows the EDS line scan of the WC–Co tool covered during the turning test by the aluminium alloy after 4-h heat treatment at 400 °C. Figure 7b presents the SEM image of the measured area. The EDS scan revealed a slight diffusion of aluminium (diffusion depth approximately 2 µm) into the cemented carbide binder phase.

Figures 8a and 9a show the EDS line scan of the TiC–FeCr and TiC–NiMo tools, respectively, covered

during the turning test by the aluminium alloy after 4-h heat treatment at 400 °C. Figures 8b and 9b present SEM images of the measured area. The EDS scan revealed a mild diffusion of aluminium (diffusion depth approximately 1 µm) into the iron- or nickel-based binder phase of the TiC-based cermets.

The diffusion of aluminium into the cobalt binder was slightly higher than its diffusion into the iron–chromium or nickel–molybdenum binder (cf. Fig. 7 and Figs 8, 9). There was no significant aluminium diffusion into the carbide phase and metallic binder diffusion into aluminium in the case of all three tested composites. At the same time, a marked diffusion of titanium but not of tungsten into aluminium was observed (cf. Fig. 7 and Figs 8, 9).

The surface failure (removal of material) during adhesive wear starts mostly in the binder by a combined

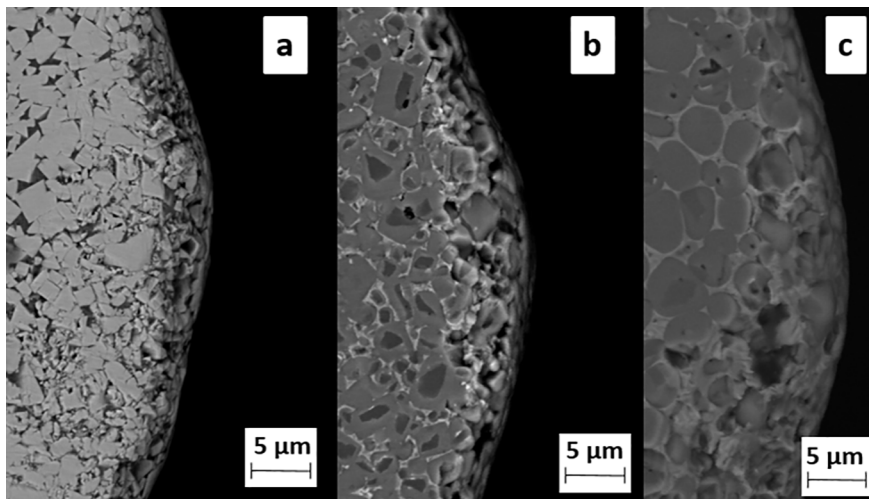


**Fig. 6.** Worn-out cutting nose tip (cutting distance 4400 m) of carbide composites WC–Co (a) and TiC–NiMo (b) and TiC–FeCr (c) cermets.

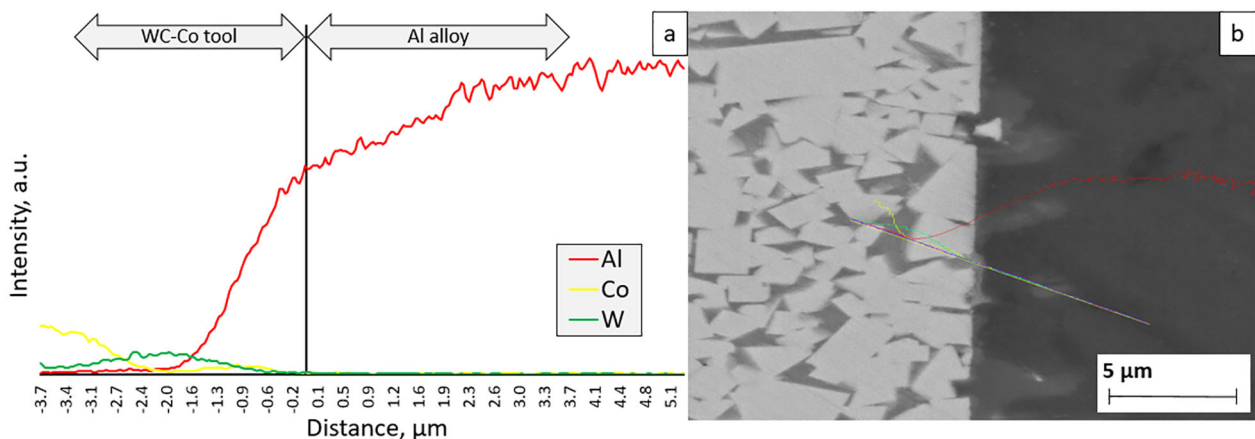


**Fig. 7.** EDS line scan (a) and the cross-section view of the WC–Co tool with a tribological layer (b).

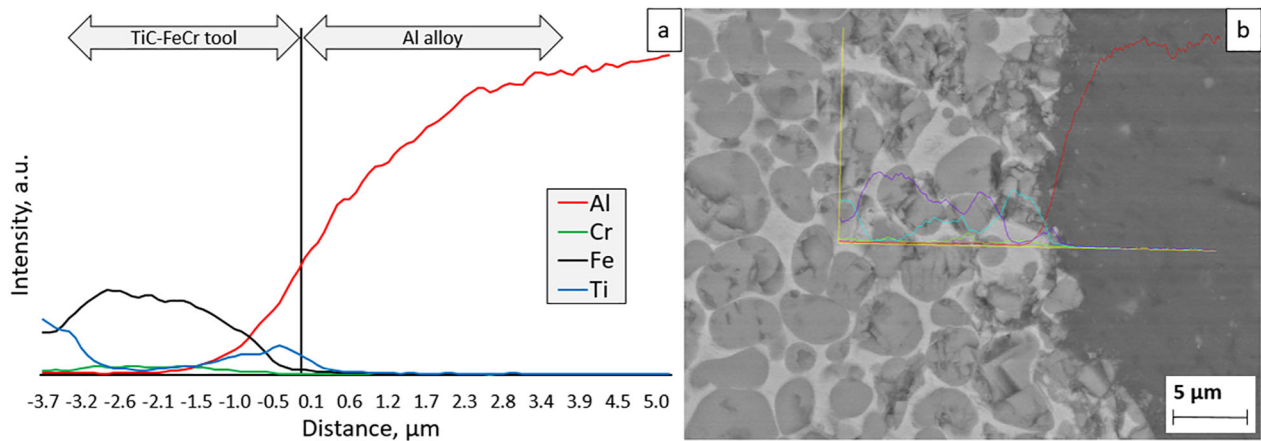


Fig. 8. EDS line scan (a) and the cross-section view of the TiC–FeCr tool with a tribological layer (b).

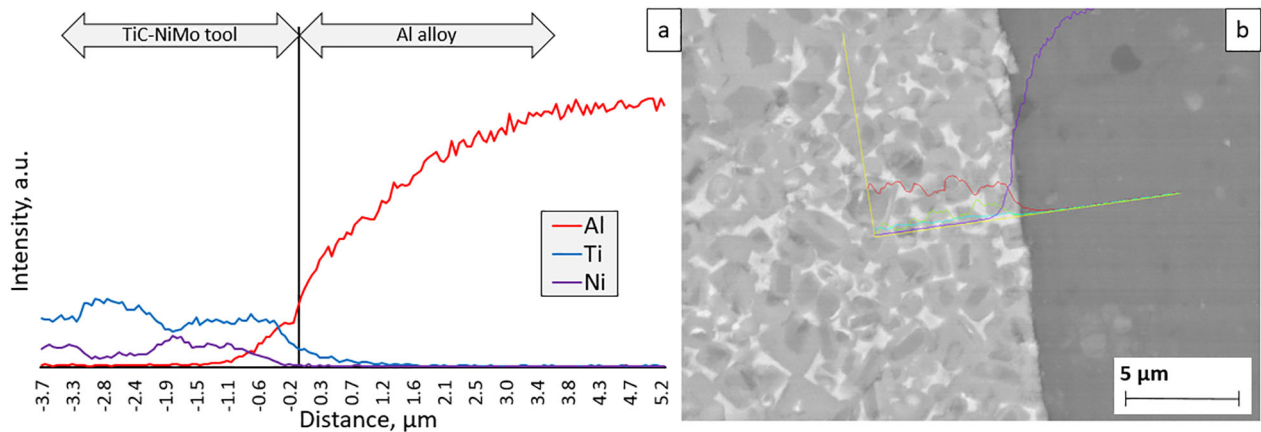


Fig. 9. EDS line scan (a) and the cross-section view of the TiC–NiMo tool with a tribological layer (b).

extrusion–extraction–microcutting process preceded by the local plastic strain that takes place prevalently in the binder of the composite. The performance of the composite in the wear conditions with predominance of adhesion depends on the carbide fraction and properties of the metallic binder. Both the increase of the volume fraction of the carbide phase in the composite and the strength of the metallic phase lead to an improvement of the adhesive wear performance of ceramic-based composites regardless of the ceramic phase composition [19]. Research of the microstructure evolution process has demonstrated that during the liquid-phase sintering of high-chromium TiC–FeCr cermets, the formation of the  $M_7C_3$  (where  $M = Cr$  and  $Fe$ ) carbide takes place in the binder region of composites [20]. As a result, the fraction of the metallic binder (Fe-based solid solution) decreases while the fraction of the carbide phase increases. An enhanced volume fraction of the carbide phase

(TiC +  $M_7C_3$ -type carbides) and a high strength of the FeCr alloy binder are predominantly behind the higher wear performance of TiC–FeCr cermets compared with WC–Co cemented carbides both at low and high temperatures (at an approximately equal TiC and WC fractions in carbide composites). The best high-temperature (400 °C) wear performance of the TiC–NiMo cermet can be attributed to the highest carbide volume fraction after sintering (see Table 1) and the high strength of the Ni-based binder at elevated temperatures.

In parallel to adhesive wear, diffusion-controlled wear takes place during FSW at high temperatures [11]. It is known that the cobalt inter-diffusion coefficient in aluminium exceeds markedly that of iron and nickel [13]. It is another aspect why ceramic-based composites with Fe- and Ni-based binders should demonstrate better wear performance at high temperatures in contact with Al than composites bonded with cobalt.

#### 4. CONCLUSIONS

The performance of carbide composites bonded with Co, Ni, and Fe alloys, in particular of cermets (TiC–NiMo and TiC–FeCr) and WC–Co cemented carbide, in wear conditions with prevailing adhesion was investigated at different temperatures (including the weld temperature during the FSW of aluminium alloys). The following conclusions were drawn:

- TiC-based cermets (TiC–NiMo, TiC–FeCr) demonstrated superiority over WC–Co cemented carbide at both low (70 °C) and elevated (400 °C) temperatures.
- The highest wear performance at the low temperature (70 °C) was demonstrated by the Fe-alloy bonded composite TiC–FeCr, while at the high temperature (400 °C) the Ni-alloy bonded cermet TiC–NiMo showed the highest performance.
- The lowest temperature sensitivity of wear resistance was demonstrated by the Ni-alloy bonded cermet TiC–NiMo.
- Enhanced high-temperature strength of the Ni-based binder as well as an increased carbide volume fraction were behind the high wear performance of the TiC–NiMo cermets.

#### ACKNOWLEDGEMENTS

This work was supported by the institutional research funding ‘Multi-scale structured ceramic-based composites for extreme applications’ (IUT 19-29) of the Estonian Research Council. The publication costs of this article were covered by the Estonian Academy of Sciences.

#### REFERENCES

1. Murr, L. E., Liu, G., and McClure, C. A TEM study of precipitation and related microstructures in friction-stir-welded 6061 aluminium. *J. Mater. Sci.*, 1998, **33**, 1243–1251.
2. Threadgrill, P. L., Leonard, A. J., Shercliff, H. R., and Withers, P. J. Friction stir welding of aluminium alloys. *Int. Mater. Rev.*, 2009, **54**, 49–93.
3. Schneider, J. A. Temperature distribution and resulting metal flow. In *Friction Stir Welding and Processing* (Misha, R. S. II and Mahoney, M. W., eds). ASM International, Materials Park, Ohio, 2007, 37–49.
4. Fuller, C. B. Friction stir tooling: tool materials and designs. In *Friction Stir Welding and Processing* (Misha, R. S. II and Mahoney, M. W., eds). ASM International, Materials Park, Ohio, 2007, 7–35.
5. Pirso, J., Juhani, K., Viljus, M., and Letunoviš, S. Two-body abrasive wear of WC-Co hardmetals in wet and dry environments. In *Proceedings of the 8th International Conference of DAAAM Baltic Industrial Engineering*, 2012, 711–716.
6. Pirso, J., Viljus, M., Letunoviš, S., Juhani, K., and Joost, R. Three-body abrasive wear of cermets. *Wear*, 2011, **271**, 2868–2878.
7. Kolnes, M., Kübarsepp, J., Sergejev, F., and Kolnes, M. Adhesive wear of WC- and TiC-based friction stir welding tool materials for aluminium alloy welding. In *Proceedings Euro PM2018*. EPMA, Pilbào, 2018.
8. Paerson, S. R., Shipway, P. H., Abere, J. O., and Hewitt, R. A. A. The effect of temperature on wear and friction of a high strength steel in fretting. *Wear*, 2013, **303**, 622–631.
9. Gåård, A., Hallbäck, N., Krakhmalev, P., and Bergström, J. Temperature effects on adhesive wear in dry sliding contacts. *Wear*, 2009, **268**, 968–975.
10. Tang, W., Guo, X., McClure, J. C., and Murr, L. E. Heat input and temperature distribution in friction stir welding. *J. Mater. Process. Manuf. Sci.*, 1998, **7**, 163–172.
11. Tarasov, S., Rubtsov, V. E., and Kolubaev, E. A. A proposed diffusion-controlled wear mechanism of alloy steel friction stir welding (FSW) tools used on an aluminum alloy. *Wear*, 2014, **318**, 130–134.
12. Alimadadi, H., Kjartansdottir, C., Burrows, A., Kasama, T., and Møller, P. Nickel-aluminum diffusion: a study of evolution of microstructure and phase. *Mater. Charact.*, 2017, **130**, 105–112.
13. Hirano, K. L., Agarwala, R. P., and Cohen, M. Diffusion of iron, nickel and cobalt in aluminum. *Acta Metall.*, 1962, **10**, 857–863.
14. Recktenwald, G. *Conversion of Thermocouple Voltage to Temperature*. Apostila, Portland, 2010.
15. De Backer, J. and Bolmsjö, G. Thermoelectric method for temperature measurement in friction stir welding. *Sci. Technol. Weld. Join.*, 2013, **18**:7, 558–565.
16. Santos, M. C. Jr., Araujo Filho, J. S., Barrozo, M. A. S., Jackson, M. J., and Macchado, A. R. Development and application of temperature measurement device using the tool-workpiece thermocouple method in turning at high cutting speeds. *Int. J. Adv. Manuf. Technol.*, 2017, **89**, 2287–2298.
17. Kübarsepp, J., Klaasen, H., and Pirso, J. Behaviour of TiC-base cermets in different wear conditions. *Wear*, 2001, **249**, 229–234.
18. Klaasen, H. and Kübarsepp, J. Abrasive wear performance of carbide composites. *Wear*, 2006, **261**, 520–526.
19. Klaasen, H., Kübarsepp, J., Roosaar, T., Viljus, M., and Traksmäa, R. Adhesive wear performance of hardmetals and cermets. *Wear*, 2010, **268**, 1122–1128.
20. Kolnes, M., Mere, A., Kübarsepp, J., Viljus, M., Maaten, M., and Tarraste, M. Microstructure evolution of TiC cermets with ferritic AISI 430L steel binder. *Powder Metall.*, 2018, **61**(3), 197–209.



## **Alumiiniumi otshõrdkeevituse tööriista potentsiaalsete materjalide kulumine keevitustemperatuuril**

Mart Kolnes, Jakob Kübarsepp, Fjodor Sergejev ja Märt Kolnes

Otshõrdkeevitus on tardfaaskeevitus, kus materjalid liidetakse mehaanilise segamise teel neid sulatamata; hõrdkeevituse temperatuur on vahemikus 400–500 °C. Otshõrdkeevituse tööriista kulumist põhjustab peamiselt adhesioonkulumine. Adhesioonkulumise uuringud viidi läbi keevitusprotsessile ligilähedasel temperatuuril, et tagada võimalikult reaalne kulumise olukord. Selleks viidi läbi adhesioonkulumise katsed, treides alumiiniumisulamit AW6082-T6 kolme erinevast materjalist tööriistaga (WC–Co, TiC–NiMo ja TiC–FeCr) madalal (70 °C) ja kõrgel (400 °C) temperatuuril. Kõrgem temperatuur saavutati löikekiiruse suurendamisega. Temperatuuri mõõtmiseks löiketsoonis kasutati uutset meetodit, mis põhineb materjalide termoelektrilisel efektil. Kulumist hinnati kui löikeriista löikeservade geomeetria muutust, kasutades skaneerivat elektronmikroskoopiat. Katsete tulemusena selgus, et TiC baasil kermistel on WC–Co kõvasulamiga võrreldes eeliseid nii madalal kui ka kõrgel keevitusprotsessi temperatuuril. Parim kulumiskindlus madalatel temperatuuridel on raua baasil sideainega TiC–FeCr kermistel ja kõrgetel temperatuuridel nikli baasil sideainega TiC–NiMo kermistel.